

# Unusual Low-Energy Phonon Dynamics in the Negative Thermal Expansion Compound $\text{ZrW}_2\text{O}_8$

Jason N. Hancock, Chandra Turpen, and Zack Schlesinger

*Physics Department, University of California Santa Cruz, Santa Cruz, CA 95064, USA*

Glen R. Kowach

*Department of Chemistry, The City College of New York, New York, NY 10031*

Arthur P. Ramirez

*Bell Laboratories, Lucent Technologies, 600 Mountain Ave, Murray Hill, NJ 07974*

(Dated: February 2, 2008)

An infrared study of the phonon spectra of  $\text{ZrW}_2\text{O}_8$  as a function of temperature which includes the low energy ( $2\text{--}10\text{ meV}$ ) region relevant to negative thermal expansion is reported and discussed in the context of specific heat and neutron density of states results. The prevalence of infrared active phonons at low energy and their observed temperature dependence are highly unusual and indicative of exotic low-energy lattice dynamics. Eigenvector calculations indicate a mixing of librational and translational motion within each low-frequency IR mode. The role of the underconstrained structure in establishing the nature of these modes, and the relationship between the IR spectra and the large negative thermal expansion in  $\text{ZrW}_2\text{O}_8$  are discussed.

The tendency of solids to expand when heated is one of the most pervasive and familiar phenomena in solid state physics[1], however, there are some compounds in which the opposite phenomenon occurs[2, 3]. In  $\text{ZrW}_2\text{O}_8$  this negative thermal expansion (NTE) is large, isotropic and persists over a broad temperature range[4, 5, 6, 7, 8, 9]. These characteristics enhance our interest in both the fundamental physics of  $\text{ZrW}_2\text{O}_8$ , and the potential applications of such a substantial NTE effect, which are widespread[3]. A defining feature of  $\text{ZrW}_2\text{O}_8$  is the existence of a 1-fold coordinated oxygen site for each  $\text{WO}_4$  tetrahedron. This terminal, or unconstrained[8], oxygen creates a structural openness along the high-symmetry  $\langle 111 \rangle$  axes and is thought to be influential in the low-energy dynamics and crucial to the phenomenon of NTE in  $\text{ZrW}_2\text{O}_8$ .

Thermal expansion phenomena generally come from anharmonic phonon dynamics[1, 6, 7, 8, 9, 10]. For  $\text{ZrW}_2\text{O}_8$  analysis of temperature dependence[7, 8, 9, 10] indicates that the low energy region should be of primary importance. To probe the low-energy phonon dynamics we use temperature dependent infrared spectroscopy covering the range from  $5000\text{ cm}^{-1}$  to  $16\text{ cm}^{-1}$  ( $600\text{--}2\text{ meV}$ ), which encompasses all the optic phonons of  $\text{ZrW}_2\text{O}_8$ . We find that the phonon-related peaks in the infrared spectra extend to unusually low energy ( $\sim 3\text{ meV}$ ), and that there is strong and unusual temperature dependence in the low-energy region, reflecting evidence of unconventional and anharmonic behavior. We suggest that understanding the mechanism of NTE and understanding the exotic nature of the infrared spectra from  $\text{ZrW}_2\text{O}_8$  are two essentially similar problems, both rooted in exotic low energy dynamics.

One of the central unresolved issues for  $\text{ZrW}_2\text{O}_8$  has to do with the nature of the eigenmode(s) responsible

for NTE. While earlier work has emphasized the role of transverse oxygen vibration[4, 5, 6, 7, 8, 9] for the mechanism of NTE, Cao et al.[11, 12] have proposed a model, based on XAFS data, in which translation of  $\text{WO}_4$  tetrahedra along  $\langle 111 \rangle$  directions plays an important role. Using eigenvector calculations together with our data, we infer that transverse oxygen motion, in the form of libration, tends to be accompanied by translation within each low-energy mode (thus they are essentially inseparable). This mixing arises due to the unconstrained oxygen and the associated openness of the structure along the high-symmetry  $\langle 111 \rangle$  direction axes, and it appears to be essential to the nature of the low-frequency IR spectra. This mixing may also be crucial to the mechanism of the NTE: while the transverse oxygen motion provides the thermal motion that contracts the lattice, the presence of a translational component in each low-energy mode provides a source of frustration that inhibits lattice instabilities that would destroy NTE.

The single-crystal samples are grown using a layered self-flux technique[13]. Our measurements of the specular reflectivity cover the frequency range from 15 to  $5000\text{ cm}^{-1}$  and the temperature range 20 to 300 K. The optical conductivity,  $\sigma(\omega)$ , is determined from the reflectivity via a Kramers-Kronig transform with carefully chosen upper and lower terminations. For the acentric  $P2_13$  structure of  $\text{ZrW}_2\text{O}_8$  one expects a total of 132 modes: 3 acoustic modes, 32 triplets of IR optical phonons, 11 doublets and 11 singlets, associated with the irreducible representations  $33T + 11E + 11A$ [14, 15, 16]. Our results are broadly consistent with earlier work[14, 15, 16, 17, 18] for the higher frequency parts of the phonon spectrum, and complementary in our emphasis on the low frequency range.

Figure 1a shows the real part of the optical conduc-

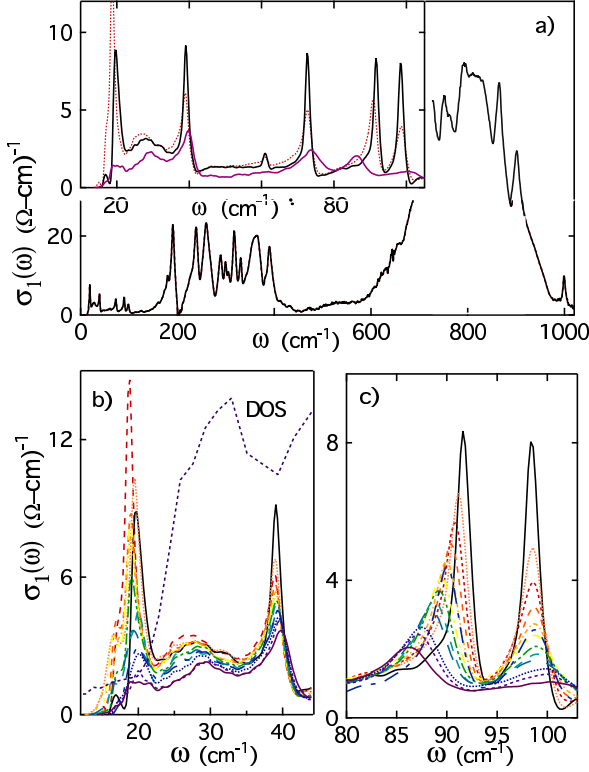


FIG. 1: (color online) a) The real part of the conductivity,  $\sigma_1(\omega)$ , is shown for the entire optic phonon region. The inset shows the low frequency region for temperatures of 20, 80 (dotted) and 240 K. b) and c) show  $\sigma_1(\omega)$  for  $T=20, 60, 80, 100, 120, 140, 160, 180, 200, 220, 240, 260$  and  $300$  K in two low  $\omega$  regions, along with neutron density of states in (b) [8]

tivity,  $\sigma_1(\omega)$ , vs frequency. The infrared active optical phonon modes, which generally appear as peaks in  $\sigma_1(\omega)$ , are sufficiently dense that they tend to merge together into clusters in  $\text{ZrW}_2\text{O}_8$ . The upper cluster is associated with bond stretching motion (including the  $\nu_3$  modes of the  $\text{WO}_4$  tetrahedra) and the middle cluster ( $180\text{--}400\text{ cm}^{-1}$ ) with bond bending modes (e.g.,  $\nu_2$  modes). Below these two clusters there are additional infrared features, shown in the inset, which we associate with librational and translational motion of  $\text{WO}_4$  tetrahedra, as discussed below. Unlike the generic modes of the upper clusters, the modes in this region are specific to the  $\text{ZrW}_2\text{O}_8$  structure, and it is in this lower region that one expects to find modes relevant to the mechanism of NTE.

As shown in Fig. 1b) and c), the peaks in this region extend to unusually low energy and exhibit striking temperature dependence. They tend to sharpen and grow in strength as the sample is cooled; they exhibit swept, asymmetric lineshapes, and in some cases substan-

tial dependence of peak frequency on temperature. The largest peak frequency shifts are observed for the broad  $28\text{ cm}^{-1}$  mode, which shifts from about  $27$  to  $29.5\text{ cm}^{-1}$  (+8%), and the  $88\text{ cm}^{-1}$  mode, which shifts from about  $91.5$  to  $86\text{ cm}^{-1}$  (-6%). These shifts are unusually large and the substantial accretion of spectral weight (presumably coming from the higher frequency) is beyond the scope of conventional phonon models. The pervasiveness of strong temperature dependence throughout this low frequency region reflects the exotic character of the low energy dynamics which is clearly evident in the IR spectra.

It is informative to consider the relationship between our IR data and specific heat [7]. For the fit shown in Figure 2a, a lowest energy Einstein mode at  $28.5\text{ cm}^{-1}$  with a spectral weight of 2.6 oscillators per unit cell provides a good fit to the leading edge of  $C(T)/T^3$  [25]. This fit is highly constraining with regard to the energy of the lowest Einstein mode; attempts to fit  $C(T)$  with a lower optical mode generate excess specific heat at low temperature as shown in Figure 2a. We therefore conclude that the  $20\text{ cm}^{-1}$  peak does not correspond to the zone-center endpoint of an ordinary optical phonon branch and that the broad  $28\text{ cm}^{-1}$  peak is the signature of the lowest optical phonon of  $\text{ZrW}_2\text{O}_8$ . The total spectral weight in the peaks between  $28$  and  $100\text{ cm}^{-1}$  is in agreement with the results of our phonon eigenvector calculations, discussed below, and the peaks in this region are in reasonable correspondence with zone-center intercepts of optical phonon dispersion relations calculated for the isostructural compound  $\text{HfW}_2\text{O}_8$  [19, 20] as well as neutron DOS peaks [8]. The  $20\text{ cm}^{-1}$  peak differs from the others in that it diminishes substantially below  $80\text{ K}$  (the others grow) and is not reconcilable with neutron DOS and  $C(T)$ . These two features may suggest a low-density defect with an extremely large dipole matrix element. Further theory is needed, in conjunction with controlled defect studies, to ascertain the origin of this marked absorption, and its possible connection with the unusual lattice dynamics of the bulk compound.

Focusing on energetics, one can let the infrared spectra provide a context in which to explore the origins of the temperature dependence of the lattice parameter,  $a(T)$ . Similar to earlier work [8, 9], we approach this by associating negative Grüneisen parameters ( $\gamma$ ) with Einstein mode frequencies. We calculate  $a(T)$  using a bulk modulus of  $72\text{ GPa}$  [21] and assuming triplet weight [1]. Starting with the frequency of the lowest optic mode from our data (at  $28\text{ cm}^{-1}=3.5\text{ meV}$ ), we find that associating a large negative Grüneisen parameter to this mode alone does not allow a good fit to  $a(T)$ , however, a good fit can be obtained simply by including a second Einstein mode at higher frequency, as shown in Figure 2b) for  $\gamma=-20$  at  $28\text{ cm}^{-1}$  and  $\gamma=-7$  at  $88\text{ cm}^{-1}$ . The lower energy corresponds to the lowest energy optical phonon in  $\text{ZrW}_2\text{O}_8$ , which is so low it cuts through the acoustic phonon dis-

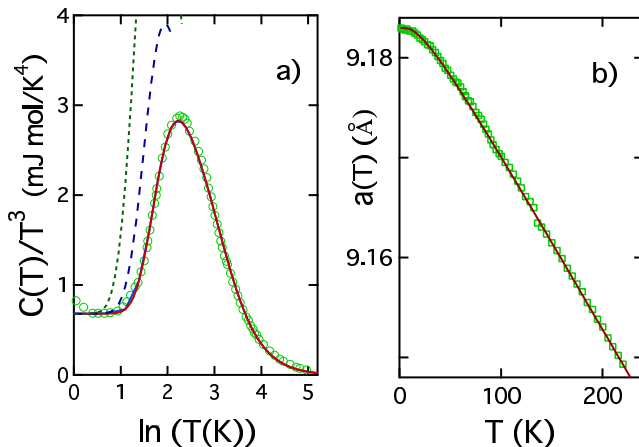


FIG. 2: (color online) a) A fit to the specific heat with a lowest infrared mode at  $28.5 \text{ cm}^{-1}$  (3.5 meV) is shown by the solid line (through the specific heat data). The dashed curves show the excess specific heat generated by failed attempts to fit  $C(T)$  with a lowest optic mode at 20 or  $24 \text{ cm}^{-1}$ , respectively. b)  $a(T)$  data (open squares) is shown along with a fit based on a two Einstein mode model.

person and may thereby acquire mixed character[20]; the higher energy corresponds to the strongly temperature dependent peak near  $88 \text{ cm}^{-1}$  (Fig 1c). While this 2-mode approach provides the minimal context in which a good fit can be obtained, one can also do more nuanced fits involving additional modes. One can use Grüneisen parameters for modes above  $40 \text{ cm}^{-1}$  from pressure dependent Raman measurements of Ravindran et al.[15] and add an additional term for the  $28 \text{ cm}^{-1}$  mode. In that more nuanced approach good fits to  $a(T)$  can be obtained when the  $\gamma$ 's of the two lowest optic modes add to about -20.

Mechanisms of NTE based on transverse thermal motion of oxygens in two-fold coordination (W-O-Zr) have been widely considered[3, 4, 5, 6, 7, 8, 9], however, Cao et al.[11, 12] have proposed an alternative model, based on XAFS data, in which translation of  $\text{WO}_4$  tetrahedra along the high-symmetry  $\langle 111 \rangle$  axes plays a key role. Ultimately the discussion of mechanism centers on the eigenvectors of the relevant phonon modes. Toward this end, we have calculated the eigenvector for each  $\mathbf{k}=0$  optical phonon mode using a mass-spring model of a 44 atom unit cell with nearest-neighbor stretching and bending interactions and periodic boundary conditions. With appropriate bond strengths, the eigenvectors exhibiting bond stretching and bending motion are associated with high ( $700\text{-}900 \text{ cm}^{-1}$ ) and moderate ( $150\text{-}400 \text{ cm}^{-1}$ ) frequency eigenvalues respectively, as expected. For the range below about  $120 \text{ cm}^{-1}$  our calculation generates 27 additional optic modes; of which 21 are associated with triplets. The two lowest energy modes are triplets at 32

and  $43 \text{ cm}^{-1}$  respectively, in reasonable correspondence with the data. The eigenvectors for these modes exhibit a mixture of librational and translational motion, as illustrated in Figure 3a. A suitable choice of eigenvector within the triplet degeneracy manifold is required to clarify the motion in this way. For the mode shown, clock-wise rotation about the  $\langle 111 \rangle$  axis is accompanied by downward translation of the two tetrahedra along the  $\langle 111 \rangle$  axis[26]

This  $\langle 111 \rangle$  axis pair is connected, via Zr-centered octahedra, to other tetrahedra as illustrated in Figure 3b. There are a total of eight  $\text{WO}_4$  tetrahedra per unit cell arranged in pairs along  $\langle 111 \rangle$  axes and offset from each other in a “spiral staircase” pattern as shown. Motion on the other  $\langle 111 \rangle$  is not the same[27] and the motions are correlated in complex ways.

This mixing of translational and rotational (librational) motion is intimately related to the underconstrained nature of the  $\text{ZrW}_2\text{O}_8$  structure, in which each tetrahedron has an unconnected (terminal) oxygen at its  $\langle 111 \rangle$  axis apex[7]. Because there are no strong second bonds for this unconstrained oxygen, translations of  $\text{WO}_4$  tetrahedra along  $\langle 111 \rangle$  axes do not involve significant bond compression and therefore project to very low frequency. There they tend to mix with the low frequency librational motion, and it is through this mixing that these low energy modes can acquire a dynamic dipole moment (since the  $\text{WO}_4$  tetrahedra carry net charge). Our observation of non-zero dipole moment for many low energy modes indicates that this mixing is pervasive. Thus the richness of the low frequency infrared spectra is connected to the existence of the unconstrained oxygen and the related openness along the high symmetry  $\langle 111 \rangle$  directions, which is a defining feature of the  $\text{ZrW}_2\text{O}_8$  structure and critical to NTE[7, 8, 9, 10, 22].

Regarding the origins of anharmonicity in  $\text{ZrW}_2\text{O}_8$ , we note that, in the context of simple harmonic picture, the uncertainties in the circumferential oxygen position would be substantial. Using the frequency of the lowest optic mode ( $28 \text{ cm}^{-1}$ ) one gets a theoretical uncertainty in the ground state of  $\Delta\theta = \sqrt{2\hbar/m_{\text{O}}r^2\omega} \simeq 14^\circ$  with a corresponding circumferential uncertainty  $\Delta(r\theta) \simeq 0.4 \text{ \AA}$ . These increase to about  $40^\circ$  and  $1.2 \text{ \AA}$  by room temperature. Such large values suggest a possible origin of anharmonicity and motivate consideration of the relevance of configurational tunneling or rotation to the low energy dynamics. Tunneling, rotation and configurational exchange phenomenon have been observed in systems with a similar 3-fold rotation axis involving methyl-group tetrahedra[23, 24], where the breakdown of the harmonic approximation for low-energy librational motion has been carefully studied. For methyl-group tetrahedra such as  $\text{CH}_3\text{I}$  the lowest librational mode frequency is typically  $80 \text{ cm}^{-1}$ , about 3 times higher than  $\text{ZrW}_2\text{O}_8$ . That most of this difference can be accounted for by the hydrogen-oxygen mass difference suggests a roughly comparable

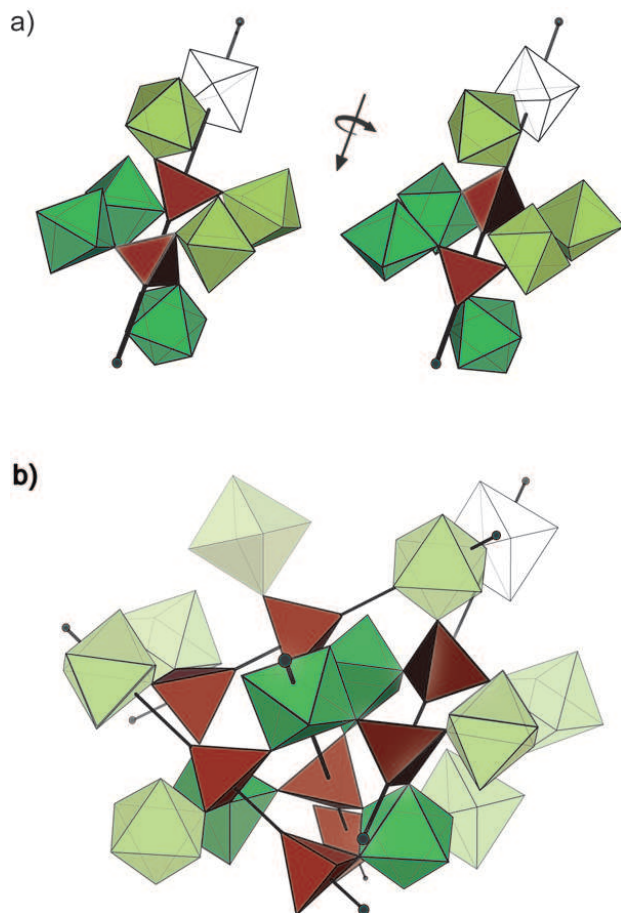


FIG. 3: (color online) a) The nature of a low frequency triplet mode is shown in terms of  $\text{WO}_4$  tetrahedra and Zr-centered octahedra via a time sequence. As the tetrahedra rotate clockwise, they translate downward along the  $\langle 111 \rangle$  axis, which is shown by the dark line. The two lowest-frequency optic mode are similar, but in the other one the  $\langle 111 \rangle$  axis octahedron (white) rotates opposite the tetrahedra. The unconstrained oxygen lies on the  $\langle 111 \rangle$  axis. b) The pair of tetrahedra shown in (a) couples to other tetrahedra as shown. There are eight  $\text{WO}_4$  tetrahedra in a unit cell organized in pairs on  $\langle 111 \rangle$  axes (dark lines) which are offset in a spiral-staircase configuration as shown. (Illustration by Alison Kendall)

confining potential to lowest order. A possible difference between  $\text{XCH}_3$  and  $\text{WO}_4$  tetrahedra arises from the nuclear spin, which is  $\frac{1}{2}$  for H, and 0 for the  $\text{O}^{16}$  nucleus, therefore a  $120^\circ$  reorientation of an  $\text{WO}_4$  tetrahedron is equivalent to a double permutation among identical particles and thus does not produce a distinct state. The potential relevance of finite barrier phenomena and large oxygen excursions to the low-energy dynamics of  $\text{ZrW}_2\text{O}_8$  remains a question for future work.

We have provided evidence for highly unusual low-energy phonon dynamics in  $\text{ZrW}_2\text{O}_8$  as reflected in our infrared spectra. We infer that the lowest optic modes in  $\text{ZrW}_2\text{O}_8$  tend to have a mixed librational and transla-

tional character in which the unconstrained oxygen plays an essential role, and it is likely that these modes play a central role in the mechanism of negative thermal expansion. While further work is needed to fully elucidate the mechanism of NTE in  $\text{ZrW}_2\text{O}_8$ , the present work shows that both librational and translational motions are operative: the transverse oxygen motion associated with libration provides NTE, while translational component within each mode frustrates a displacive transition that would otherwise remove the unique structural environment in which these mixed phonon modes exist.

We gratefully acknowledge F. Bridges, D. Cao, O. Narayan and W.E. Pickett for helpful conversations. Work at UCSC supported by NSF Grant DMR-0071949.

- 
- [1] N. W. Ashcroft and N. D. Mermin, *Solid State Physics* (Saunders College, 1976).
  - [2] G. K. White, *Contemporary Physics* **34**, 193 (1993).
  - [3] A. W. Sleight, *Current Opinion in Solid State and Materials Science* **3**, 128 (1998).
  - [4] T. A. Mary, J. S. O. Evans, T. Vogt, and A. W. Sleight, *Science* **272**, 90 (1996).
  - [5] J. S. O. Evans, T. A. Mary, T. Vogt, M. Subramanian, and A. W. Sleight, *Chem. Mater.* **8**, 2809 (1996).
  - [6] A. K. A. Pryde, K. D. Hammonds, M. T. Dove, V. Heine, J. D. Gale, and M. C. Warren, *J. Phys. Cond. Matt.* **8**, 10973 (1996).
  - [7] A. P. Ramirez and G. R. Kowach, *Phys. Rev. Lett.* **80**, 4903 (1998).
  - [8] G. Ernst, C. Broholm, G. R. Kowach, and A. P. Ramirez, *Nature* **396**, 147 (1998).
  - [9] W. I. F. David, J. S. O. Evans, and A. W. Sleight, *Europhys. Lett.* **46**, 661 (1999).
  - [10] R. Mittal and S. L. Chaplot, *Phys. Rev. B* **60**, 7234 (1999).
  - [11] D. Cao, F. Bridges, G. R. Kowach, and A. P. Ramirez, *Phys. Rev. Lett.* **89**, 215902/1 (2002).
  - [12] D. Cao, F. Bridges, G. R. Kowach, and A. P. Ramirez, *Phys. Rev. B* **68**, 14303 (2003).
  - [13] G. R. Kowach, *J. Cryst. Growth* **212**, 167 (2000).
  - [14] T. R. Ravindran, A. K. Arora, and T. A. Mary, *Phys. Rev. Lett.* **84**, 3879 (2000).
  - [15] T. R. Ravindran, A. K. Arora, and T. A. Mary, *Journal of Physics: Condensed Matter* **13**, 11573 (2001).
  - [16] B. Chen, D. V. S. Muthu, Z. X. Liu, A. W. Sleight, and M. B. Kruger, *Phys. Rev. B* **64**, 214111/1 (2001).
  - [17] Y. Yamamura, N. Nakajima, T. Tsuji, M. Koyano, Y. Iwasa, S. Katayama, K. Saito, and M. Sorai, *Phys. Rev. B* **66**, 014301/1 (2002).
  - [18] T. R. Ravindran, A. K. Arora, and T. A. Mary, *Phys. Rev. B* **67**, 64301 (2003).
  - [19] R. Mittal, S. L. Chaplot, H. Schober, and T. A. Mary, *Phys. Rev. Lett.* **86**, 4692 (2001).
  - [20] R. Mittal, S. L. Chaplot, A. I. Kolesnikov, C. K. Loong, and T. A. Mary, *Phys. Rev. B* **68**, 54302 (2003).
  - [21] J. D. Jorgensen, Z. Hu, S. Teslic, D. N. Argyriou, S. Short, J. S. O. Evans, and A. W. Sleight, *Phys. Rev. B* **59**, 215 (1999).

- [22] S. Allen and J. S. O. Evans, Phys. Rev. B **68**, 134101 (2003).
- [23] M. Prager and A. Heidemann, Chem. Rev. **97**, 2933 (1997).
- [24] R. M. Dimeo, Am. J. Phys. **71**, 885 (2002).
- [25] The fit includes a  $\Theta_D = 62\text{ cm}^{-1}$  and Einstein contributions at IR and Raman peak frequencies above  $28\text{ cm}^{-1}$ .
- [26] For most parameter choices, this is one of the two lowest energy modes. In the other the  $\langle 111 \rangle$ -axis octahedra rotates opposite to the two tetrahedra. Two singlet modes with purely translational motion (along the  $\langle 111 \rangle$  axes) also occur at relatively low frequencies which are sensitive to weak next-nearest-neighbor interactions.
- [27] The motion includes librations in which the unconstrained oxygens tilt away from their  $\langle 111 \rangle$  axes.